Davis Catherine Van Wie (Orcid ID: 0000-0003-4279-5369)
Ontiveros Cuadras Jorge Feliciano (Orcid ID: 0000-0002-8550-1036)
Benitez-Nelson Claudia R. (Orcid ID: 0000-0002-1004-5048)
Schmittner Andreas (Orcid ID: 0000-0002-8376-0843)
Tappa Eric J. (Orcid ID: 0000-0002-2142-5820)
Osborne Emily (Orcid ID: 0000-0001-9579-5851)
Thunell Robert (Orcid ID: 0000-0001-7052-1707)

Ongoing increase in Eastern Tropical North Pacific denitrification as interpreted through the Santa Barbara Basin sedimentary $\delta^{15}N$ record

C. V. Davis[1], J. F. Ontiveros-Cuadras[2], C. Benitez-Nelson[1], A. Schmittner[3], E. J. Tappa[1], E. Osborne[4], R. C. Thunell[1,†]

[1] School of the Earth, Ocean, and Environment, University of South Carolina
[2] Instituto de Ciencias del Mar y Limnología, Universidad Nacional Autónoma de México
[3] College of Earth, Ocean, and Atmospheric Sciences, Oregon State University
[4] Ocean Acidification Program, National Oceanic and Atmospheric Administration
[†] Deceased: July 30, 2018

Corresponding author: Catherine V. Davis (cvdavis@seoe.sc.edu)

Key Points:

- Nitrogen isotopes of bulk sediment in Santa Barbara Basin are seasonally variable and reflect the influence of Eastern Tropical North Pacific waters
- Multiannual and decadal-scale variability in nitrogen isotopes are partially influenced by local processes
- Nitrogen isotope records suggest that modern day Eastern Tropical North Pacific denitrification is higher than during the past 2000 years

This article has been accepted for publication and undergone full peer review but has not been through the copyediting, typesetting, pagination and proofreading process which may lead to differences between this version and the Version of Record. Please cite this article as doi: 10.1029/2019PA003578

Abstract

Decades of observations show that the world's oceans have been losing oxygen, with far-reaching consequences for ecosystems and biogeochemical cycling. To reconstruct oxygenation beyond the limited scope of instrumental records, proxy records are needed, such as sedimentary $\delta^{15}N$. We combine two $\delta^{15}N$ records from the Santa Barbara Basin (SBB), a 24-year long, biweekly sediment trap time series, and a 114-year, high-resolution sediment core together spanning the years 1892-2017. These records allow for the examination of $\delta^{15}N$ variability on seasonal to centennial timescales. Seasonal variability in SBB $\delta^{15}N$ is consistent in timing with the poleward advection of a high $\delta^{15}N$ signal from the Eastern Tropical North Pacific in the summer and fall. Strong El Niño events result in variable $\delta^{15}N$ signatures, reflective of local rainfall, and neither the Pacific Decadal Oscillation nor North Pacific Gyre Oscillation impose strong controls on bulk sedimentary $\delta^{15}N$. Seasonal and interannual variability in sediment trap $\delta^{13}C_{org}$ is consistent with local productivity as a driver, however this signal is not retained in the sediment core. The time series from the sediment trap and core show that bulk sedimentary $\delta^{15}N$ in SBB has now exceeded that measured for the past 2000 years. We hypothesize that the change in $\delta^{15}N$ reflects the increasing influence of denitrified waters from the Eastern Tropical North Pacific and ongoing deoxygenation of the Eastern Pacific. When juxtaposed with other regional $\delta^{15}N$ records our results further suggest that SBB is uniquely situated to record long-term change in the Eastern Tropical North Pacific.

1. Introduction

Oxygen deficient zones (ODZs) are critical to global biogeochemical cycling (Breitburg et al., 2018; Gruber, 2008) and changes in the expanse and intensity of ODZs have profound implications for marine life and ocean geochemistry (Breitburg et al., 2018; Levin, 2017; Stramma et al., 2010b; Stramma et al., 2012). ODZs have expanded globally over the past several decades (Breitburg et al., 2018; Levin, 2017; Keeling et al., 2009; Stramma et al., 2008). However, instrumental records of oxygenation are sparse and too short to adequately address oxygen variability on geologic timescales or differentiate between decadal oscillations and longer-term trends. Understanding longer-term temporal variability in marine oxygenation must therefore rely on sedimentary proxy records (e.g., Deutsch et al., 2014; Emmer and Thunell, 2000; Kienast et al., 2002; Liu et al., 2005).

The Eastern Tropical North Pacific (ETNP) hosts one of the largest expanses of oxygen depleted waters (Karstensen et al., 2008; Paulmier and Ruiz-Pino, 2009) and a suite of reactions that influence global nitrogen cycling (DeVries et al., 2012; Liu et al., 2005). Under oxygen deficient conditions microbial activity converts bioavailable nitrate (NO_3^-) to nitrogen (N_2), a process referred to as denitrification, and both removes bioavailable nitrogen and imposes an N isotopic fractionation as ^{14}N is preferentially consumed. As a result, the the residual NO_3^- pool in the ETNP has a ratio of ^{15}N to ^{14}N ($(^{15}N/^{14}N)_{sample}/(^{15}N/^{14}N)_{atmosphere}$ - 1) *1000 or $\delta^{15}N$) that is substantially higher (> 15‰) than typical open ocean values of 4 - 6‰ (Brandes et al., 2003; Sigman et al., 1997; Sigman and Casciotti, 2001; Sigman et al., 2009; Voss et al., 2001). The high $\delta^{15}N$ signature of the ETNP is transported northward within the California Under Current (CUC) and is observed in both the water column and sediments as far north as Vancouver Island, Canada (Altabet et al., 1999; Castro et al., 2001; Chang et al., 2008; Kienast et al., 2002; Liu and Kaplan, 1989). Thus the Eastern Pacific margin provides

an important long-term record of denitrification in the ETNP (Altabet et al., 1999; Deutsch et al., 2014; Emmer and Thunell, 2000; Tems et al., 2015; Thunell and Kepple, 2004). Sedimentary $\delta^{15}N$, however, may be influenced by local as well as distal sources as was demonstrated in the San Pedro Basin (Collins et al., 2011). This may complicate the interpretation of sedimentary $\delta^{15}N$ as a proxy for denitrification in the ETNP.

Latitudinal comparisons of sediments show that the $\delta^{15}N$ decreases along the Eastern Pacific margin with increasing distance from the ETNP (Kienast et al., 2002) and that temporal variability in the relative strength of the CUC may impact local $\delta^{15}N$ records (Tems et al., 2015). Less is known as to the extent that regional overprinting may influence individual records. Interpreting ODZ expansion may be especially complicated in upwelling boundary zones such as the California Current System (CCS) where changes in upwelling and productivity are likely to accompany oscillations in regional and global climatology (e.g., Bakun, 1990, 2015; García-Reyes et al., 2015; Sydeman et al., 2014; Varela et al., 2015). Local upwelling can decrease subsurface oxygen due to the physical upwelling of high nutrient water masses that promote increased productivity at the surface and respiration at depth. Further complexities may occur in regions such as Santa Barbara Basin (SBB), California, where anoxic bottom and pore waters allow periodic denitrification to occur within the basin (Goericke et al., 2015; Liu and Kaplan, 1989; Sigman et al., 2003). Thus in SBB, sedimentary $\delta^{15}N$ variability may represent a combined influence of the magnitude of ETNP water transport, mixing with other water masses, local nutrient utilization or denitrification, terrestrial inputs, and regional oceanography (Figure 1). Emmer and Thunell (2000) showed that SBB sediment cores record the high $\delta^{15}N$ signal associated with ETNP denitrification on millennial time scales. Using sinking particles collected by deep moored sediment traps (1993-1994), they also found that bulk sedimentary $\delta^{15}N$ was highest during

upwelling. This suggests that regional processes may influence SBB sedimentary $\delta^{15}N$ records and raises questions as to the relative importance of local versus distal sources on sedimentary $\delta^{15}N$ in SBB and the timescales over which they are relevant.

In order to disentangle the timescales of varying influences on the SBB bulk $\delta^{15}N$ sediment record, we reexamine the now ~24-year long moored sediment trap time series of sinking particle $\delta^{15}N$ from SBB along with a sediment core dated from 1892 to 2006 (Osborne et al., 2016). The aim of the study is to evaluate seasonal, interannual, and decadal influences on bulk sedimentary $\delta^{15}N$ in the basin over the past 125-years. To further constrain potential influences on $\delta^{15}N$ due to local oceanography and changes in productivity, we have also generated a record of the carbon isotopic composition of organic material ($\delta^{13}C_{org}$ defined as $((^{13}C/^{12}C)_{sample}/(^{13}C/^{12}C)_{VPDB} - 1) *1000$) from both the sediment trap time series and sediment core.

Santa Barbara Basin is located just south of the Southern California Bight and is bordered to the north by California, U.S.A, and to the south by the Channel Islands. The flow within the 590 m deep basin is restricted by sills at ~230 m depth to the east and ~480 m to the west (Talley, 1993; Figure 2). Low oxygen source waters, restricted flow, and high productivity (and thus respiration) leave the modern SBB anoxic below the western sill throughout most of the year. Anoxic conditions may be temporarily relieved by occasional "flushing" events associated with intense upwelling near Point Conception in spring or winter (Bograd et al., 2002; Goericke et al., 2015; Reimers et al., 2003). A combination of deep basin anoxia and a high sedimentation rate result in laminated sediments and ideal conditions for paleoceanographic reconstructions (e.g., Cannariato et al., 1999; Emmer and Thunell, 2000; Hendy and Kennett, 1999; Nederbragt et al., 2008).

Seasonality in SBB is driven by upwelling-favorable winds along the California coastline. In the spring, upwelling brings cold, nutrient-rich waters to the surface, initiating phytoplankton blooms dominated by diatoms (Anderson et al., 2008; Brzezinski and Washburn, 2011; Dorman and Winant, 1999; Harms and Winant, 1998; Hendershott and Winant, 1996; Otero and Siegel, 2004; Figure 3). By fall, upwelling-favorable winds relax, resulting in an overall decrease in productivity and surface water warming (Anderson et al., 2008; Dorman and Winant, 1999; Hendershott and Winant, 1996; Otero and Siegel, 2004; Thunell, 1998; Figure 3). Flow through SBB is poleward for much of the year with a strong influence of the CUC/Inshore Counter Current systems fed by equatorial waters (Bray et al., 1999; Chelton, 2012; Lynn and Simpson, 2012; Figure 2). The dominant direction of surface flow reverses during the spring upwelling period (~February-June) with an increased influence of the California Current and North Pacific Intermediate Waters (Bray et al., 1999; Harms and Winant, 1998; Hickey, 1979; Lynn and Simpson, 1987). Upwelling events at or north of Point Conception are associated with the blocking of poleward flow over the eastern sill (Hickey, 1992). Given its shallow eastern sill, on-shelf location, and that the main branch of the CUC is located offshore at > 250 m, the majority of poleward flow through SBB is likely derived from the Inshore Counter Current. In practice, the definitions and loci of these flows are variable and the entire system of poleward flow as it influences SBB is referred to here as the California Counter Current (CCC).

2. Methods

2.1 Sediment trapping time series

Data collection from the SBB sediment trap time series began in 1993 and data are currently available through 2017. Sinking particles for $\delta^{15}N$ and $\delta^{13}C$ analyses were collected from a sediment trap moored near the center of SBB (34°14′N, 120°02′W; Figure 2) using an

automated McLane Labs 13-cup sediment trap with a 0.5 m diameter aperture. Biweekly trap samples have been collected nearly continuously since initiation of the project with traps redeployed every ~6 months. Our record relies primarily on the sediment trap located around 500 m depth (~90 m above the seafloor). Over the course of the ~24-year time series the trap position has ranged from 409 to 532 m. A second "shallow" sediment trap was deployed from late 2010 to 2017 between 146 and 289 m depth. In a few cases, due to malfunction or insufficient material collected in the "deep" trap, material from the "shallow" trap was substituted into our $\delta^{13}C_{org}$ (but not $\delta^{15}N$) time series to allow for a more complete record (noted in Supplementary Data and discussed further below). Until 2015 sediment traps were poisoned with 10 g L^{-1} sodium azide. Starting in 2015 an 8% formalin solution has been used to poison and preserve material in the lower trap. No step change occurs in either $\delta^{15}N$ or $\delta^{13}C$ coincident with the change in preservation method used (Supplemental Figure 1).

2.2 Multi-core collection and processing

Multicore SBB-MC1-DB (34°13′N, 119°58′W; 580 m depth; Figure 1) was collected from SBB in 2012. The core was sampled at 0.5 cm resolution up to 10 cm depth and then at 1 cm resolution to 50 cm. Lead 210 and cesium 137 were used to date the core and to develop an age model ±1 year (Osborne et al., 2016).

2.3 Isotopic analyses

Analyses of sediment trap $\delta^{15}N$ and $\delta^{13}C_{org}$ were conducted on a quarter split of trap material that was freeze-dried and ground. Samples for $\delta^{13}C_{org}$ analyses were further acidified to remove inorganic $\delta^{13}C$. Fluxes of C and N were measured as weight percent on a Perkin Elmer 2400 CHNS/O Elemental Analyzer and are reported in g m^{-2} day^{-1} based on the dry weight of total flux to the trap. Homogenized sediments of 30-60 ug for N or 80-110 ug for C

were run on an Isoprime isotope ratio mass spectrometer coupled to a VG Isoprime IRMS at the University of South Carolina (with a lower detection mass 20 ug for both $\delta^{15}N$ and $\delta^{13}C_{org}$). Results for $\delta^{15}N$ are reported relative to atmospheric N_2 (0‰) and $\delta^{13}C_{org}$ relative to VPDB. Standard reference materials were analyzed at the beginning and end of each run (~30 samples) with NIST RM-8542, NIST RM-8541, NIST RM-8542, and USGS 40 used for $\delta^{13}C_{org}$, and IAEA-N-1, IAEA-N-2, IAEA-N0-3, and USGS40 used for $\delta^{15}N$. Between 2 and 4 replicates of a single homogenized sample were run every ~20 samples and produced an average standard error of 0.1‰ for $\delta^{13}C_{org}$ and 0.040‰ for $\delta^{15}N$. A difference of < 0.67‰ was measured for all $\delta^{13}C_{org}$ replicates, and < 0.21‰ for all $\delta^{15}N$ replicates.

2.4 Data processing and sources

All hydrologic data, including temperature, density, and nutrient data were sourced from openly available datasets, primarily from the monthly Plumes and Blooms time series (http://www.oceancolor.ucsb.edu/plumes_and_blooms/; accessed on 17-06-2019), which has sampled mid-SBB hydrography to 100 m since 1996. Local rainfall data are available on the Santa Barbara County website (http://www.countyofsb.org/pwd/rainhistory.sbc, accessed on 30-06-2018). Determinations as to the phase and state of the El Niño Southern Oscillation (ENSO), Pacific Decadal Oscillation (PDO), and North Pacific Gyre Oscillation (NPGO) were based on the Oceanic Niño Index (ONI), and data available at http://jisao.washington.edu/pdo/PDO.latest (accessed on 30-04-2018) and http://www.o3d.org/npgo/ (accessed on 15-04-2019) respectively. Data on total Organic Carbon (TOC), terrigenous, and opal fluxes to the sediment trap are also available as described in Thunell et al. (2007).

2.5 Modeling

We used the University of Victoria (UVic, version 1.9) climate model coupled to the Model of Ocean Biogeochemistry and Isotopes (MOBI, version 1.4) as described in more detail in Schmittner and Lund (2015). The global UVic model includes a three-dimensional ocean component at a coarse resolution (1.8×3.6º, 19 vertical levels), a simple single-layer atmospheric Energy-Moisture-Balance-Model, which uses a prescribed monthly climatology of winds, and a dynamic-thermodynamic sea ice model. MOBI1.4 includes two classes of phytoplankton (nitrogen fixers and a general non-nitrogen-fixing phytoplankton class), one class of zooplankton, detritus, and nitrate and phosphate as limiting nutrients. It simulates nitrogen isotopes (^{15}N and ^{14}N) separately in all compartments of its interactive nitrogen cycle including fractionation during denitrification in the water column and in sediments, and the isotopic effects of nitrogen fixation (Somes et al., 2017). UVic/MOBI was driven only with historical CO_2 emissions from 1750 to the present. Its simulated decadal mean atmospheric CO_2 in 2000-2010 is 378 ppm compared with observations from Mauna Loa of 380 ppm (Dr. Pieter Tans, NOAA/ESRL, www.esrl.noaa.gov/gmd/ccgg/trends/ accessed on 30-10-2018). Model global surface air temperature increased between 1890-1900 and 2000-2010 by 0.66ºC, close to observational estimates of 0.82ºC (GISTEMP Team, 2018; Hansen et al., 2010).

2.6 Statistics

All statistics were carried out using the R software base package (R Core Team, 2010) and the *PMCMRplus* package (Pohlert, 2018). Assumptions of normality were not met by $\delta^{15}N$ and $\delta^{13}C_{org}$ data, identified by a Shapiro-Wilk test (Shapiro and Wilk, 1965). The non-parametric Kruskal-Wallis test (Kruskal and Wallis, 1952) and a Dunn post-hoc test (Dunn,

1964) were used to assess seasonality of $\delta^{15}N$ and $\delta^{13}C_{org}$ as defined by the start date of trap collection for each sample.

3. Results

3.1 Seasonality of $\delta^{15}N$ and $\delta^{13}C$

A large amount of stochastic variability, but limited seasonality, was observed in the flux of $\delta^{15}N$ to the deep SBB sediment trap. Only the $\delta^{15}N$ of samples collected beginning in March was found to be significantly lower than samples collected in August and September ($p < 0.05$; Figure 4). Similarly, months with the highest $\delta^{13}C_{org}$ values (April-May) are significantly different than those with the lowest values (October -January) (Figure 5). The total C and N fluxes are highest in traps opening June (Supplementary Data) and there is a weak positive relationship between C flux and $\delta^{13}C_{org}$ ($R^2 = 0.15$, $p < 0.012$). While a positive correlation between $\delta^{15}N$ and $\delta^{13}C_{org}$ in sediment trap samples is statistically significant, it is not meaningful ($R^2 = 0.01$, $p = 0.02$).

In the most recent available year of overlapping shallow and deep sediment trap data (2016-2017) $\delta^{13}C_{org}$ values were positively correlated between the two traps ($R^2 = 0.65$, $p < 0.001$). Differences in $\delta^{15}N$ between the shallow and the deep trap, however, vary depending on the depth of the shallow trap. From October 2010 to June 2015, the shallow trap was deployed between 137 and 146 m with a mean $\delta^{15}N$ of 8.9‰ ±1.1. There was no systematic offset from values recorded in the deep trap (averaging 8.4‰ ±1.1 over the same interval). Subsequent to June 2015, the shallow trap depth was lowered to between 239 and 289 m, and had a $\delta^{15}N$ that averaged 7.8‰ ±0.4 between June 2015 and October 2017. This was significantly lower than the average $\delta^{15}N$ of 9.3‰ ±1.0 measured in the deep trap over the same time period (Supplementary Figure 1; Kruskal-Wallis; chi-squared =63.01, $p < 0.001$).

3.2 Long-term trends in SBB $\delta^{15}N$ and $\delta^{13}C_{org}$

The 114-year down-core $\delta^{15}N$ record ranges between 6.7‰ and 8‰. A decrease in $\delta^{15}N$ of roughly 0.5‰ occurs from the 1890s into the 1920s (Figure 6). Between the 1920s and 1990s $\delta^{15}N$ is consistently between 6.7 and 7.4‰. A rapid increase in $\delta^{15}N$ begins in the mid-1990s with values reaching 8‰ in 2005 and 2006, higher than at any previous point in the record. In contrast, there is no trend in the sediment core $\delta^{13}C_{org}$ record, which ranges from -22.8‰ to -21.3‰ between 1894 and 2006 (Figure 7).

3.3 Comparison of sediment trap and core records of $\delta^{15}N$ and $\delta^{13}C_{org}$

The biweekly sediment trap time series of both $\delta^{13}C_{org}$ and $\delta^{15}N$ display more variability than down-core records and are reflective of seasonal and stochastic variability. Results comparing flux-weighted annual $\delta^{15}N$ from the sediment trap and age-paired sediment samples show only a minimal offset of ~0.5‰ with core material having lower $\delta^{15}N$ values than sediment trap material (Supplemental Figure 2). Flux weighted annual records also closely approximate both the absolute values and the trends observed in down-core records when there is temporal overlap (Figure 6). Combined, sediment trap and core data represent a continuous high-resolution record of SBB bulk sedimentary $\delta^{15}N$ from 1892 to 2017. The overlay of the sediment trap $\delta^{15}N$ record with down core record supports the larger scale shift seen in both with an increase of ~3‰ occurring between the mid 1990s and 2017.

Unlike the $\delta^{15}N$ record, comparison between sediment trap and down-core $\delta^{13}C_{org}$ indicates a poor match between the carbon isotopic composition of the sediment trap time series and core measurements. Down-core carbon isotope values are 0.5-1‰ higher than observed during comparable intervals from the sediment traps (Supplemental Figure 2). This is a substantial offset given the fairly small range of down-core $\delta^{13}C_{org}$ values (-22.8 to -21.2‰).

3.4 ENSO-driven variability in $\delta^{15}N$ and $\delta^{13}C$

Oceanic Niño Index values indicate the occurrence of two "strong" (> 1.5 °C sea surface temperature anomaly) El Niño events over the course of the sediment trap time series, the first in 1997/1998 and the second in 2015/2016. Several strong La Niña events were captured in 1998-2000, 2007/2008 and 2010-2012 (Figure 8). Additional years characterized by weaker El Niño or La Niña conditions were also sampled. The relationship between ENSO phases and sediment trap $\delta^{15}N$ values is inconsistent. During the 1997/1998 El Niño, $\delta^{15}N$ values are generally lower, especially through the fall and winter, whereas in 2015/2016, $\delta^{15}N$ are higher than average (Figure 8; Supplemental Figure 3). Years with dominant La Niña conditions do not display markedly different $\delta^{15}N$ signals, except in the 1995/1996 La Niña, where $\delta^{15}N$ was higher throughout the year than in either the proceeding or following years (Figure 8; Supplemental Figure 3).

The sediment trap record of $\delta^{13}C_{org}$, in contrast, is significantly lower during strong and moderate El Niño years when compared with La Niña or neutral years (Kruskal-Wallis; chi-squared =26.20, $p < 0.001$) (Figure 8; Supplemental Figure 3). Neither $\delta^{15}N$ nor $\delta^{13}C_{org}$ show any significant relationship with periods of strong or all periods of ENSO activity in down-core records (Kruskal-Wallis; $p = 0.84$ and $p = 0.32$ respectively). However, even small uncertainties in sediment dating and the inevitable averaging across multiple years could obscure a down-core ENSO signal.

3.5 Potential for influence of PDO or NPGO on stable isotope signals

Both PDO and NPGO have varied with similar phasing over the course of the sediment trap time series. Two documented regime shifts have occurred in PDO; the first from a warm to a cool phase in ~2000 and then a return to a warm phase in ~2016. Shifts between positive and

negative phasing of the NPGO have occurred in 1998, 2005, 2007, and 2014. The $\delta^{13}C_{org}$ recorded over the sediment trap time series is significantly higher during the cool phase of the PDO (Kruskal-Wallis; chi-squared =14.39, $p < 0.001$) and positive phase of the NPGO (Kruskal-Wallis; chi-squared =17.07, $p < 0.005$). Sediment trap $\delta^{15}N$ is not significantly different during different NPGO phasing (Kruskal-Wallis; $p = 0.74$), and potential trends in $\delta^{15}N$ associated with shifts in PDO phase are obscured by the overall increase of ~ 3‰ observed over this same time period. Down-core, cool PDO phases are significantly higher in $\delta^{15}N$ (Kruskal-Wallis; chi-squared =7.57, $p = 0.006$). This significance disappears when years after 1995 are excluded ($p = 0.13$) suggesting that the rapid increase in $\delta^{15}N$ experienced since the mid-1990s cool PDO phase dominates the long-term signal.

4. Discussion

4.1 Upwelling drives seasonal signals in $\delta^{13}C_{org}$

The seasonal signal of $\delta^{13}C_{org}$ observed in the deep SBB sediment trap suggests that it is driven by local changes in productivity. The increase in $\delta^{13}C_{org}$ in the spring through summer coincides with phytoplankton blooms in SBB, initiated by the presence of nutrient rich upwelled waters (Thunell, 1998; Figure 3). This increase is also consistent with a decrease in fractionation that occurs with increased phytoplankton growth rates (Burkhardt et al., 1999; Francois et al., 2012; Fry, 1996; Fry and Wainright, 1991; Laws et al., 1995; Popp et al., 1998). The full seasonal range of $\delta^{13}C_{org}$ falls within reported values for marine phytoplankton (Deines, 1980; Meyers, 1994), It should be noted that terrestrial end members near SBB have very similar $\delta^{13}C_{org}$ to those observed in the sediment trap suggesting that sedimentary $\delta^{13}C_{org}$ is likely a poor tracer for the relative influences of marine and terrestrial sources in SBB (Figure 1; Sarno et al., *this issue*).

The lower $\delta^{13}C_{org}$ observed in the sediment core compared to the sediment trap points to a relatively rapid alteration of the $\delta^{13}C_{org}$ signal (Figure 7). A similarly altered $\delta^{13}C_{org}$ signal has been shown previously to result from both oxic and anoxic degradation in freshwater (Lehmann et al., 2002), although no such offset was observed between sediment trap and core top samples in the Gulf of California (Pride et al., 1999). We hypothesize that in SBB this offset is most likely due to the addition of material with a lower $\delta^{13}C_{org}$ value, such as from sediment microbial communities. For example, *Beggiatoa* mats have been identified in the deep SBB (Bernhard et al., 2003), which can have a $\delta^{13}C_{org}$ signature as low as -28‰ when influenced by hydrocarbons (Zhang et al., 2005). As no $\delta^{13}C_{org}$ trend is observed in the upper portion of the core (Figure 7), the alteration of the $\delta^{13}C_{org}$ signal can be assumed to be both rapid (occurring within the 6 years between the most recent sample and core recovery) and persistent. This is in contrast to the $\delta^{13}C$ of foraminiferal shells from the same core, which preserve a negative $\delta^{13}C$ trend associated with increased upwelling and CO_2 in SBB (Osborne, 2016). Thus, despite the close ties between productivity and $\delta^{13}C_{org}$ found in sediment trap samples, changes in $\delta^{13}C_{org}$ on the order of 1-2‰ are unlikely to reflect changes in productivity or export in the SBB sediment core record.

4.2 Transport from the ETNP overwhelms local $\delta^{15}N$ signals on annual timescales

The bulk $\delta^{15}N$ in sediment cores collected from along the Eastern Pacific margin is primarily a reflection of poleward advection of the ETNP $\delta^{15}N$ signal (Altabet et al., 1999; Castro et al., 2001; Chang et al., 2008; Emmer and Thunell, 2000; Kienast et al., 2002; Liu and Kaplan, 1989). In SBB the highest $\delta^{15}N$ values occur during the early fall, when poleward advection is highest (Bray et al., 1999; Harms and Winant, 1998; Hickey, 1979, 1992; Lynn and Simpson, 1987, 2012). These results are similar to those found off the Oregon coast, where higher sedimentary $\delta^{15}N$ values were observed during periods of increased poleward transport

(Kienast et al., 2002). Indeed, the lowest $\delta^{15}N$ values in SBB occur in the spring when poleward transport is lowest or absent (Bray et al., 1999; Harms and Winant, 1998; Hickey, 1979, 1992; Lynn and Simpson, 1987, 2012). We note that while nitrogen utilization is complete in SBB surface waters for most of the year, it is also during spring upwelling that NO_3 availability may increase in surface waters (Figure 3). Incomplete NO_3 utilization in surface waters would be expected to further decrease the $\delta^{15}N$ of sinking material.

Differences in the $\delta^{15}N$ signature between the surface and deep sediment trap time series suggest a depth dependent change in the $\delta^{15}N$ of sinking particles in the water column (Supplemental Figure 1). When the shallow trap was located between 130 and 146 m, $\delta^{15}N$ values were higher than those measured during the same period in the deep trap at > 400 m. However, after the shallow trap was moved deeper to between 239 and 289 m, $\delta^{15}N$ signatures became less variable and lower than those recorded simultaneously in the deep trap or previously at shallower depths. The clear step change of 1.1‰ that occurs between 146 and 239 m indicates the presence of a more complicated $\delta^{15}N$ profile in SBB. A decrease in $\delta^{15}N$ of sinking material has also been observed in other basins, although at much greater depths (e.g. Altabet, 1991, 1988; Voss et al., 1996; Freudenthal et al., 2001).

Our findings differ somewhat from the interpretations of Emmer and Thunell (2000), but not with their conclusion that an ETNP source dominates the long-term $\delta^{15}N$ record in the basin. The earlier study is based on the first year and a half of sediment trap $\delta^{15}N$ (1993-1994) and shows higher $\delta^{15}N$ values during a period of upwelling. The extended time series, however, reveals overall lower $\delta^{15}N$ observed in association with the spring upwelling season, and highlights the importance of multi-decadal time series in interpreting sedimentary proxies. It

also provides a mechanism (i.e., seasonal advection) by which the SBB $\delta^{15}N$ record reflects ETNP denitrification on multiannual timescales.

Only modest differences between core top and deep sediment trap $\delta^{15}N$ have been observed across the Eastern Pacific margin from Monterey Bay to the Gulf of California (Altabet et al., 1999; Robinson et al., 2012), including in SBB (Prokopenko et al., 2006). This is reaffirmed by our results that show only a small (0.5‰) offset between the deep sediment trap and sedimentary $\delta^{15}N$ (Supplemental Figure 2), and a comparable record of $\delta^{15}N$ increase in the two archives (Figure 6). In SBB, an increase in the $\delta^{15}N$ of nitrate has previously been observed in the water column beneath the depth of the eastern sill and oxic boundary at > 500 m (Sigman et al., 2003). This is not reflected in the difference in bulk $\delta^{15}N$ between the deep sediment trap and the sediment core. We therefore conclude that the signal of $\delta^{15}N$ flux observed in the deep sediment trap is largely preserved in SBB sediments.

4.3 Interannual variability from ENSO and PDO

4.3.1 ENSO

No evidence was found for coherent and significant variations in bulk sedimentary $\delta^{15}N$ due to ENSO variability, with differences in $\delta^{15}N$ records between the 1997 and 2015 El Niño event potentially attributable to variations in rainfall and terrestrial $\delta^{15}N$ inputs (Figure 8; Jong et al., 2018; Lee et al., 2018; Sarno et al., *this issue*; Sweeney and Kaplan, 1980). A decrease in sediment trap $\delta^{13}C_{org}$ is associated with both El Niño events. This is consistent with an interpretation of sediment trap $^{13}C_{org}$ as reflecting a decrease in productivity associated with El Niño along the California margin (Figure 8; Supplemental Figure 3; Chavez, 1996; Thunell, 1998).

4.3.2 PDO and NPGO

The PDO may have an influence on $\delta^{15}N$ records via changes in thermocline depth in the ETNP (Deutsch et al., 2011) and in water mass transport (Tems et al., 2015). No clear relationship between $\delta^{15}N$ and PDO phasing is observed either in our sediment trap record or down-core, once the record after 1995 is excluded. Similarly, no relationship is noted between $\delta^{15}N$ and the more recently defined NPGO Index (Di Lorenzo et al., 2008). The sediment trap record of $\delta^{13}C_{org}$ does indicate significantly higher values associated with cool PDO and positive NPGO phases over the past 24 years, which again may reflect increased upwelling and greater productivity, as shown by previous work (Bringué et al., 2014; Mantua et al., 1997; Di Lorenzo et al., 2008; Nezlin et al., 2017).

4.4 Increase in $\delta^{15}N$ from the 1990s to present

A dramatic ~3‰ increase in sedimentary $\delta^{15}N$ has occurred in SBB between the 1990s and 2017, such that sedimentary $\delta^{15}N$ in SBB is now unprecedentedly high for the past 2000 years over which high-resolution $\delta^{15}N$ records are available (Wang et al., *this issue*; Figure 6). Comparable records from Santa Monica Basin (Figure 9c), Soledad Basin, and Pescadaro Basin (Supplemental Figure 2), all capture the beginning of this trend, and reflect changes in the ETNP (Deutsch et al., 2014; Tems et al., 2015). The ETNP ODZ has expanded over the past few decades (Deutsch et al., 2014; Horak et al., 2016; Stramma et al., 2008, 2010a) and the observed increase in $\delta^{15}N$ likely reflects an increase in denitrification in the ETNP.

Increases in $\delta^{15}N$ are not only associated with an expanding ETNP ODZ, but also oxygen loss along the California Margin (Bograd et al., 2008, 2015; Deutsch et al., 2014; Goericke et al., 2015; McClatchie et al., 2010; Tems et al., 2015), in the Southern California Bight, and SBB (Bograd et al., 2008, 2015; Goericke et al., 2015; McClatchie et al., 2010; Tems et al., 2015).

Meanwhile, the contribution of Pacific Equatorial Waters to the CUC may be increasing and shifting northward (Meinvielle and Johnson, 2014). The combination of an increase in $\delta^{15}N$ values within the ETNP (Duetsch et al., 2014; Tems et al., 2015), decreased disolved oxygen in source waters to the CCC (Bograd et al., 2008, 2015), and an increased equatorial influence on CCC waters (Meinvielle and Johnson, 2014) all implicate a southern source for the increase in SBB $\delta^{15}N$ observed over the past three decades.

In addition to broader regional trends, Goericke et al. (2015) describe a decrease in nitrate concentrations in the deep SBB since 1986. Based on quarterly California Cooporative Oceanic Fisheries Investigations (CalCOFI) data, biochemical changes in SBB are attributed to a decrease in the frequency of the occasional, upwelling-associated flushing events that refresh the oxygen depleted region of the basin below the western sill. While, we find no direct evidence to link flushing events to the sediment trap $\delta^{15}N$ record, a long-term decrease in ventilation would also promote increased water column denitrification, and potentially contribute to an increasing trend in sedimentary $\delta^{15}N$.

4.5 SBB $\delta^{15}N$ records reflect long-term anthropogenic changes

In order to examine the possibility of anthropogenic forcing as a driver of the recent increase in sedimentary $\delta^{15}N$, a modeling exercise was conducted using UVic/MOBI, focused on the expected change in $\delta^{15}N$ of nitrate in the ETNP since the 1880s. The model uses static wind forcing and lacks a resolved Counter Current that transports water poleward along the Eastern Pacific margin. Thus the output functions as an estimate of anthropogenically-forced changes in the $\delta^{15}N$ of nitrate in the ETNP and shows a meaningful increase in $\delta^{15}N$ as a consequence of anthropogenic CO_2 occurring over the past 125 years (Figure 9). The $\delta^{15}N$ anomaly of both modeled ETNP $\delta^{15}N$ flux and the SBB record are similar in magnitude and timing since the

1920s (Figure 9). To distinguish this trend from additional non-anthropogenic drivers, the modeled trend was removed from the SBB record (Figure 9). Subtraction of this long-term trend reveals a mid-century $\delta^{15}N$ minimum in SBB similar to that observed in southern records such as the Santa Monica Basin (Figure 9c; Deutsch et al., 2014; Tems et al., 2015), as well as the decrease of ~1‰ measured from the late 1800s to the 1950s. The mid-century minimum described in other records has been linked to decadal-scale variability in Walker circulation and trade wind strength, resulting in a contraction of the ETNP ODZ (Cheung et al., 2016; Deutsch et al., 2014). Thus, comparison with both neighboring basins and modeled ETNP $\delta^{15}N$ strongly implies that increasing $\delta^{15}N$ in SBB is the product of both decadal scale variability (via Walker circulation) and longer-term anthropogenic forcing.

The mid-century divergence between SBB sedimentary $\delta^{15}N$ and the records previously published by Deutsch et al. (2014) and Tems et al. (2015), suggests a dampening of decadal-scale variability in SBB and a more anthropogenically-forced record. In the 1990s a global shift from "zonal" to "meridional" wind patterns occurred, with the later associated with stronger trade winds over the tropical North Pacific, stronger North Pacific gyre circulation, and stronger upwelling along the California margin (as reviewed by Oviatt et al., 2015) and in the ETNP. Thus, prior to the mid-1990s, a deeper thermocline and smaller ODZ in the ETNP may have been accompanied by decreased North Pacific gyre strength and decreased upwelling (relative to modern) off of Point Conception. Reduced gyre strength would be expected to increase the relative influence of the CCC compared to the CC (Tems et al., 2105), increasing poleward transport of a high $\delta^{15}N$ signal. However, an additional mechanism specific to SBB is required to explain the difference between centennial $\delta^{15}N$ records from SBB and Santa Monica Basin.

Upwelling around Point Conception has been shown to block equatorward flow through SBB (Hickey, 1992). Therefore, we hypothesize that reduced upwelling off of Point Conception could allow greater poleward movement specifically through SBB, providing an additional mechanism to obscure a mid-century decrease in $\delta^{15}N$ advected poleward from the ETNP. Few records are available prior to the 1950s, however, the Pacific Fisheries Upwelling Index shows reduced upwelling north of Point Conception at 36°N from the 1960s to the mid-1990s when compared to present conditions (Figure 9a). This is roughly coincident with a dominant positive PDO phase, and the period of greatest discrepancy between the SBB sediment record and the trends observed farther south (Supplemental Figure 4). The well-documented increase in Central California upwelling over the past three decades, attributable to anthropogenic impacts and/or multi-decadal oscillations (García-Reyes and Largier, 2010; Jacox et al., 2014; Oschlies et al., 2018; Seo et al., 2012), further supports reduced mid-century upwelling compared to the modern day. In parallel, a decrease in the strength of upwelling activity near Point Conception would decrease the frequency of flushing events in SBB and increase the potential for local denitrification. It should be noted that earlier intervals of decoupling between SBB Pescadero Basin $\delta^{15}N$ records have also been documented and attributed to large-scale perturbations in North Pacific circulation (Wang et al., *this issue*).

While apparent discrepancies between SBB and other Eastern Pacific Margin sites may pose a limitation on the interpretation of decadal-scale variability in the sedimentary $\delta^{15}N$ record, our findings support an interpretation of the SBB record as reflecting longer term ETNP ODZ expansion as proposed by Emmer and Thunell (2000). Moreover, our results indicate that the SBB offers a more faithful record of the long-term anthropogenically forced component of ETNP denitrification.

5. Conclusions

Stable isotopes of $\delta^{15}N$ and $\delta^{13}C_{org}$ from bulk sinking particles display seasonality in their flux to the SBB. Sub-annual variability in water column $\delta^{13}C_{org}$ is driven by productivity, but the down-core bulk $\delta^{13}C_{org}$ record is subject to rapid alteration in the sediment. Seasonality in bulk $\delta^{15}N$ reflects poleward advection of the $\delta^{15}N$ of nitrate from the ETNP. Applying this interpretation to the substantial increase in $\delta^{15}N$ observed in sediment trap and core records since the 1990s leads to the conclusion that as of 2017, the extent of ETNP denitrification is greater than in the past 2000 years. While the long-term signal of sedimentary $\delta^{15}N$ appears to reflect tropical processes, multiannual (ENSO) to multidecadal variability is partially overprinted by the influences of local rainfall and upwelling, making the SBB record distinct from neighboring basins. Thus, the record of $\delta^{15}N$ in SBB is best interpreted as representing long-term trends in the ETNP ODZ. The apparent dampening of decadal-scale signals may prove useful in disentangling the influence of anthropogenic forcing on ODZ expansion from natural short-term oscillations. The recent increase in bulk $\delta^{15}N$ in SBB cannot be explained by decadal oscillations or local factors, and likely represents a long-term increase in ETNP denitrification driven by anthropogenic climate change.

Acknowledgements

Many thanks to I. Hendy for comments on an early version of this manuscript and to P. Rafter and an anonymous reviewer for their constructive reviews. We are grateful to the captain and crew of the *R/V Shearwater* and all of the alumni of the Thunell Marine Sediment Research Laboratory who assisted in the collection and processing of sediment trap samples over several decades. This work was supported by NSF OCE 1631977 (R.C.T. and C.B.), NSF 1634719 (A.S.), and Consejo Nacional de Ciencia y Tecnología grant I0010-2015-01 (J.F.O). Nitrogen and organic carbon isotope data from the sediment trap can be found in the

supplement to this manuscript, and in the BCO-DMO database (https://www.bco-dmo.org/dataset/773318/data).

References

Altabet, M.A. (1988) Variations in nitrogen isotopic composition between sinking and suspended particles: implications for nitrogen cycling and particle transformation in the open ocean. *Deep-Sea Research I*, 35(4): 535-554.

Altabet, M. A., Pilskaln, C., Thunell, R., Pride, C., Sigman, D., Chavez, F., & Francois, R. (1999). The nitrogen isotope biogeochemistry of sinking particles from the margin of the Eastern North Pacific. *Deep Sea Research Part I: Oceanographic Research Papers*, 46(4), 655-679.

Anderson, C. R., Siegel, D. A., Brzezinski, M. A., & Guillocheau, N. (2008). Controls on temporal patterns in phytoplankton community structure in the Santa Barbara Channel, California. *Journal of Geophysical Research*, 113, C04038. doi:10.1029/2007JC004321.

Bakun, A. (1990), Global climate change and intensification of coastal ocean upwelling. *Science*, 247(4939), 198-201.

Bakun, A., Black, B., Bograd, S. J., Garcia-Reyes, M., Miller, A., Rykaczewski, R., & Sydeman, W. (2015). Anticipated effects of climate change on coastal upwelling ecosystems. *Current Climate Change Reports*, 1(2), 85-93.

Banaru, D., Carlotti, F., Barani, A., Gregori, G., Neffati, N., & Harmelin-Vivien, M. (2014). Seasonal variation of stable isotope ratios of size-fractionated zooplankton in the Bay of Marseille (NW Mediterranean Sea). *Journal of Plankton Research*, 36(1),145-156.

Bernhard, J. M., Visscher, P. T., & Bowser, S. S. (2003). Submillimeter life positions of bacteria, protists, and metazoans in laminated sediments of the Santa Barbara Basin. *Limnology and Oceanography*, 48, 813-828.

Bode, A. & Alvarez-Ossorio, M. T. (2004). Taxonomic versus trophic structure of mesozooplankton: a seasonal study of species succession and stable carbon and nitrogen isotopes in a coastal upwelling ecosystem. *ICES Journal of Marine Science*, 61(4), 563-571.

Bograd, S. J., Chereskin Teresa, K., & Roemmich, D. (2001). Transport of mass, heat, salt, and nutrients in the southern California Current System: Annual cycle and interannual variability. *Journal of Geophysical Research: Oceans*, 106, 9255-9275.

Bograd, S. J., Schwing Franklin, B., Castro Carmen, G., & Timothy David, A. (2002). Bottom water renewal in the Santa Barbara Basin. *Journal of Geophysical Research: Oceans*, 107, 3216-3225. http://doi.org/10.1029/2001JC001291

Bograd, S. J., Castro, C. G., Di Lorenzo, E., Palacios, D. M., Bailey, H., Gilly, W., & Chavez, F. P. (2008). Oxygen declines and the shoaling of the hypoxic boundary in the California Current. *Geophysical Research Letters*, 35. http://doi.org/10.1029/2008GL034185

Bograd, S. J., Buil, M., Di Lorenzo, E., Castro, C. G., Schroeder, I. D., Goericke, R., Anderson, C. R., Benitez-Nelson, C., & Whitney, F. A. (2015) Changes in source waters to the Southern California Bight. *Deep-Sea Research II*, 112, 42-52.

Brandes, J. A., Devol Allan, H., Yoshinari, T., Jayakumar, D. A., & Naqvi, S. W. A. (2003). Isotopic composition of nitrate in the central Arabian Sea and eastern tropical North Pacific: A tracer for mixing and nitrogen cycles. *Limnology and Oceanography*, 43(7), 1680-1689.

Bray, N. A., Keyes, A., & Morawitz, W. M. L. (1999). The California Current system in the Southern California Bight and the Santa Barbara Channel. *Journal of Geophysical Research: Oceans*, 104, 7695-7714.

Breitburg, D., Levin, L. A., Oschlies, A., Grégoire, M., Chavez, F. P., Conley, D. J., et al. (2018). Declining oxygen in the global ocean and coastal waters. *Science*, 359(6383), 1475-1476.

Bringué, M., Pospelova, V., & Field, D. B. (2014). High resolution sedimentary record of dinoflagellate cysts reflects decadal variability and 20th century warming in the Santa Barbara Basin. *Quaternary Science Reviews*, 105, 86-101.

Brzezinski, M. A. & Washburn, L. (2011). Phytoplankton primary productiviy in the Santa Barbara Channel: Effects of wind-driven upwelling and mesoscale eddies. *Journal of Geophysical Research*, 116(C12013). http://doi.org/10.1029/2011JC007397

Burkhardt, S., Riebesell, U., & Zondervan, I. (1999). Effects of growth rate, CO_2 concentration, and cell size on the stable carbon isotope fractionation in marine phytoplankton. *Geochimica et Cosmochimica Acta*, 63(22), 3729-3741.

Cannariato, K. G., Kennett, J. P., & Behl, R. J. (1999). Biotic response to late Quaternary rapid climate switches in Santa Barbara Basin: Ecological and evolutionary implications. *Geology*, 27(1), 63-66.

Castro, C., Chavez, F., & Collins, C. (2001). Role of the California Undercurrent in the export of denitrified waters from the eastern tropical North Pacific. *Global Biogeochemical Cycles*, 15(4), 819-830.

Chang, A. S., Pedersen, T. F., & Hendy, I. L. (2008). Late Quaternary paleoproductivity history on the Vancouver Island margin, western Canada: a multiproxy geochemical study. *Canadian Journal of Earth Sciences*, 45(11), 1283-1297.

Chavez, F. P. (1996). Forcing and biological impact of onset of the 1992 El Niño in central California. *Geophysical Research Letters*, 23(3), 265-268.

Chelton, D. B., Bernal, P., & McGowan, J. A. (1982). Large-scale interannual physical and biological interaction in the California Current. *Journal of Marine Research*, 40(4), 1095-1125.

Chelton, D. B. (2012). Seasonal variability of alongshore geostrophic velocity off central California. *Journal of Geophysical Research: Oceans*, 89(C3), 3473-3486.

Cheung, W. W., Frölicher, T. L., Asch, R. G., Jones, M. C., Pinsky, M. L., Reygondeau, G., et al. (2016). Building confidence in projections of the responses of living marine resources to climate change. *ICES Journal of Marine Science*, 73(5), 1283-1296.

Collins, L.E., Berelson, W., Hammond, D.E., Knapp, A., Schwartz, R. & Capone, D. (2011) Particle fluxes in San edro Basin, California: A four-year record of sedimentation and physical forcing. *Deep-Sea Research I*, 58: 898-914.

Deines, P. (1980). The isotopic composition of reduced organic carbon. In J. C. Fontes, (Eds.), *The Terrestrial Environment* (pp. 329-406). Amsterdam, Elsevier.

Deutsch, C., Berelson, W., Thunell, R., Weber, T., Tems, C., McManus, J., et al. (2014). Centennial changes in North Pacific anoxia linked to tropical trade winds. *Science*, 345(6197), 665-668.

Deutsch, C., Brix, H., Ito, T., Frenzel, H., & Thompson, L. (2011). Climate-forced variability of ocean hypoxia. *Science*, 333(6040), 336-339.

Dever, E. P., & Winant, C. D. (2002) The evolution and depth structure of shelf and slope temperatures and velocities during the 1997–1998 El Niño near Point Conception, California. *Progress in Oceanography*, 54(1), 77-103.

DeVries, T., Deutsch, C., Primeau, F., Chang, B., & Devol, A. (2012). Global rates of water-column denitrification derived from nitrogen gas measurements. *Nature Geoscience*, 5(8), 547-550.

Di Lorenzo, E., Schneider, N., Cobb, K.M., Franks, P.J.S., Chhak, K., Miller, A.J., McWilliams, J.C., Bograd, S.J., Arango, H., Churchitser, E., Powell, T.M., & Riviere, P. (2008) North Pacific Gyre Oscillation links ocean climate and ecosystem change. *Geophysical Research Letters*, 35, L08607, doi:10.1029/2007GL032838.

Dorman, C. E., & Winant, C. D. (1999). The structure and variability of the marine atmosphere around the Santa Barbara Channel. *Monthly Weather Review*, 128, 261-282.

Dunn, O.J. (1961) Multiple comparisons using rank sums, *Technometrics*, 6: 241-252.

Emmer, E., & Thunell, R. C. (2000). Nitrogen isotope variations in Santa Barbara Basin sediments: Implications for denitrification in the eastern tropical North Pacific during the last 50,000 years. *Paleoceanography*, 15(4), 377-387.

Francois, R., Altabet Mark, A., Goericke, R., McCorkle Daniel, C., Brunet, C., & Poisson, A. (2012) Changes in the δ13C of surface water particulate organic matter across the subtropical convergence in the SW Indian Ocean. *Global Biogeochemical Cycles*, 7(3), 627-644.

Freudenthal, T., Neuer, S., Meggers, H., Davenport, R., & Wefer, G. (2001) Influence of lateral particle advection and organic matter degredation on sediment accumulation and stable nitrogen isotope ratios along a productivity gradient in the Canary Islands region. *Marine Geology*, 177: 93-109.

Fry, B. (1996) $^{13}C/^{12}C$ fractionation by marine diatoms. *Marine Ecology Progress Series*, 134(1-3), 283-294.

Fry, B., & Wainright, S. C. (1991). Diatom sources of ^{13}C-rich carbon in marine food webs. *Marine Ecology Progress Series*, 76(2), 149-157.

García-Reyes, M., Sydeman, W. J., Schoeman, D. S., Rykaczewski, R. R., Black, B. A., Smit, A. J., & Bograd, S. J. (2015). Under pressure: Climate change, upwelling, and eastern boundary upwelling ecosystems. *Frontiers in Marine Science*, 2(109). http://doi.org/10.3389/fmars.2015.00109

García-Reyes, M., & Largier, J. (2010). Observations of increased wind-driven coastal upwelling off central California. *Journal of Geophysical Research: Oceans*, 115(C4). http://doi.org/10.1029/2009JC005576

Gay, P. S., & Chereskin Teresa, K. (2009). Mean structure and seasonal variability of the poleward undercurrent off southern California. *Journal of Geophysical Research: Oceans*, 114(C2). http://doi.org/10.1029/2008JC004886

GISTEMP Team, 2018: GISS Surface Temperature Analysis (GISTEMP). NASA Goddard Institute for Space Studies. Dataset accessed 2018-10-30 at https://data.giss.nasa.gov/gistemp/.

Goericke, R., Bograd, S. J., & Grundle, D. S. (2015). Denitrification and flushing of the Santa Barbara Basin bottom waters. *Deep Sea Research Part II: Topical Studies in Oceanography*, 112, 53-60.

Gruber, N. (2008). The marine nitrogen cycle: overview and challenges. In D. G. Capone, D. A. Bronk, M. R. Mulholland, & J. C. Carpenter (Eds.), *Nitrogen in the Marine Environment* (Vol. 2, pp. 1-50). Academic Press.

Hansen, J., Ruedy, R., Sato, M., & Lo, K. (2010). Global surface temperature change, *Reviews of Geophysics*, 48, RG4004. http://doi.org/10.1029/2010RG000345.

Harms, S., & Winant, C. D. (1998). Characteristic patterns of the circulation in the Santa Barbara Channel. *Journal of Geophysical Research: Oceans*, 103(C2), 3041-3065.

Hendershott, M. C., & Winant, C. D. (1996). Surface circulation in the Santa Barbara Channel. *Oceanography,* 9(2), 114–121. https://doi.org/10.5670/oceanog.1996.14.

Hendy, I. L., & Kennett, J. P. (1999). Latest Quaternary North Pacific surface-water responses imply atmosphere-driven climate instability. *Geology*, 27(4), 291-294.

Hertz, E., Trudel, M., Carrasquilla-Henao, M., Eisner, L., Farley, E. V., Moss, J. H., Murphy, J M., & Mazumder, A. (2018). Oceanography and community structure drive zooplankton carbon and nitrogen dynamics in the eastern Bering Sea. *Marine Ecology Progress Series*, 601(97-108). https://doi.org/10.3354/meps12647

Hickey, B. M. (1979). The California Current system—hypotheses and facts. *Progress in Oceanography*, 8(4), 191-279.

Hickey, B. M. (1992). Circulation over the Santa Monica-San Pedro basin and shelf. *Progress in Oceanography*, 30(1-4), 37-115.

Horak, E. A., Ruef, W., Ward Bess, B., & Devol Allan, H. (2016). Expansion of denitrification and anoxia in the eastern tropical North Pacific from 1972 to 2012. *Geophysical Research Letters*, 43(10), 5252-5260.

Jacox, M. G., Moore, A. M., Edwards, C. A., & Fiechter, J. (2014). Spatially resolved upwelling in the California Current System and its connections to climate variability. *Geophysical Research Letters*, 41(9), 3189-3196.

Jong, B.-T., Ting, M., Seager, R., Henderson, N., & Lee, D. E. (2018), Role of Equatorial Pacific SST forecast error in the late winter California precipitation forecast for the 2015/16 El Niño. *Journal of Climate*, 31(2), 839-852.

Karstensen, J., Stramma, L., & Visbeck, M. (2008). Oxygen minimum zones in the eastern tropical Atlantic and Pacific oceans. *Progress in Oceanography*, 77(4), 331-350.

Keeling, R. F., Körtzinger, A., & Gruber, N. (2009) Ocean deoxygenation in a warming world. *Annual Review of Marine Science*, 2(1), 199-229.

Kienast, S. S., Calvert, S. E., & Pedersen, T. F. (2002). Nitrogen isotope and productivity variations along the northeast Pacific margin over the last 120 kyr: Surface and subsurface paleoceanography. *Paleoceanography*, 17(4). https//doi.org/10.1029/2001PA000650

Kruskal, W.H., & Wallis, A. (1952) Use of ranks in one-criterion variance analysis, *Journal of the American Statistical Association*, 47: 583-621.

Laws, E. A., Popp, B. N., Bidigare, R. R., Kennicutt, M. C., & Macko, S. A. (1995). Dependence of phytoplankton carbon isotopic composition on growth rate and $[CO_2]_{aq}$: Theoretical considerations and experimental results. *Geochimica et cosmochimica acta*, 59(6), 1131-1138.

Lee, S. K., Lopez, H., Chung, E. S., DiNezio, P., Yeh, S. W., & Wittenberg Andrew, T. (2018) On the fragile relationship between El Niño and California rainfall. *Geophysical Research Letters*, 45(2), 907-915.

Lehmann, M. F., Bernasconi, S. M., Barbieri, A., & McKenzie, J. A. (2002). Preservation of organic matter and alteration of its carbon and nitrogen isotope composition during simulated and in situ early sedimentary diagenesis. *Geochimica et Cosmochimica Acta*, 66(20), 3573-3584.

Levin, L. (2017). Manifestation, drivers, and emergence of open ocean deoxygenation. *Annual Review of Marine Science*, 10, 229-260. https://doi.org/10.1146/annurev-marine-121916-063359

Liu, K. K., & Kaplan, I. R. (1989). The eastern tropical Pacific as a source of ^{15}N-enriched nitrate in seawater off southern California. *Limnology and Oceanography*, 34(5), 820-830.

Liu, Z., Altabet Mark, A., & Herbert Timothy, D. (2005). Glacial-interglacial modulation of eastern tropical North Pacific denitrification over the last 1.8-Myr. *Geophysical Research Letters*, 32, L23607. https://doi.org/10.1029/2005GL024439

Lorenzen, C. J. (1967). Vertical distribution of chlorophyll and phaeo-pigments: Baja California. *Deep Sea Research*, 14, 735-745.

Lynn, R. J., & Simpson, J. J. (1987). The California Current system: The seasonal variability of its physical characteristics. *Journal of Geophysical Research: Oceans*, 92(C12), 12947-12966.
Lynn, R. J., & Simpson, J. J. (2012). The flow of the undercurrent over the continental borderland off southern California. *Journal of Geophysical Research: Oceans*, 95(C8), 12995-13008.
Mantua, N. J., Hare, S. R., Zhang, Y., Wallace, J. M., & Francis, R. C. (1997). A Pacific interdecadal climate oscillation with impacts on salmon production. *Bulletin of the american Meteorological Society*, 78(6), 1069-1079.
Mantua, N.J., The Pacific Deacadal Oscillation (PDO), http://research.jisao.washington.edu/pdo/, Latest Access: December 2, 2018.
McClatchie, S., Goericke, R., Cosgrove, R., Auad, G., & Vetter, R. (2010). Oxygen in the Southern California Bight: Multidecadal trends and implications for demersal fisheries. *Geophysical Research Letters*, 37, L19602. doi:10.1029/2010GL044497
Meinvielle, M., & Johnson, G. C. (2014). Decadal water-property trends in the California Undercurrent, with implications for ocean acidification. *Journal of Geophysical Research: Oceans*, 118(12), 6687-6703.
Meyers, P. A. (1994). Preservation of elemental and isotopic source identification of sedimentary organic matter. *Chemical Geology*, 114(3), 289-302.
Nederbragt, A. J., Thurow, J. W., & Bown, P. R. (2008). Paleoproductivity, ventilation, and organic carbon burial in the Santa Barbara Basin (ODP Site 893, off California) since the last glacial. *Paleoceanography*, 23(1), PA1211.
Nezlin N. P., McLaughlin, K., Booth, J. A. T., Cash, C. L., Diehl D. W., Davis K. A., et al. (2017). Spatial and temporal patterns of chlorophyll concentration in the Southern California Bight. *Journal of Geophysical Research: Oceans*, v. 123(1), 231-245.
Osborne, E. B., Thunell, R. C., Marshall, B. J., Holm, J. A., Tappa, E. J., Benitez-Nelson, C., Cai, W., & Chen, B. (2016) Calcification of the planktonic foraminifera Globigerina bulloides and carbonate ion concentration: Results from the Santa Barbara Basin. *Paleoceanography*. http://doi.org/10.1002/2016PA002933
Osborne, E. B. (2016) Development and application of foraminiferal carbonate system proxies to quantify ocean acidificaiton in the California Current, PhD Dissertation, University of South Carolina, Columbia, South Carolina.
Otero, M. P. & Siegel, D. A. (2004). Spatial and temporal characteristics of sediment plumes and phytoplankton blooms in the Santa Barbara Channel, *Deep-Sea Research II*, 51, 1129-1149.
Oviatt, C., Smith, L., McManus, M. C., & Hyde, K. (2015). Decadal patterns of westerly winds, temperatures, ocean gyre circulations and fish abundance: A review. *Climate*, 3(4), 833-857.
Paulmier, A., & Ruiz-Pino, D. (2009). Oxygen minimum zones (OMZs) in the modern ocean. *Progress in Oceanography*, 80(3–4), 113-128.
Pohlert, T. (2018). Calculate pairwise multiple comparisons of mean rank sums. http://CRAN.R-project.org/package=PMCMRplus.
Popp, B. N., Laws, E. A., Bidigare, R. R., Dore, J. E., Hanson, K. L., & Wakeham, S. G. (1998). Effect of phytoplankton cell geometry on carbon isotopic fractionation. *Geochimica et Cosmochimica Acta*, 62(1), 69-77.
Pride, C., Thunell, RC., Sigman, D., Keigwin, L., Altabet, M. & Tappa, E. (1999) Nitrogen isotopic variations in the Gulf of California since the last deglaciation: Response to global climate change. *Paleoceanography*, 14(3): 397-409.
Prokopenko, M., Hammond, D., Berelson, W., Bernhard, J., Stott, L., & Douglas, R. (2006). Nitrogen cycling in the sediments of Santa Barbara basin and Eastern Subtropical

North Pacific: Nitrogen isotopes, diagenesis and possible chemosymbiosis between two lithotrophs (Thioploca and Anammox)—"riding on a glider". *Earth and Planetary Science Letters*, 242(1), 186-204.

Reimers, C. E., Lange C. B., Tabak, M., & Bernhard J. M. (2003). Seasonal spillover and varve formation in the Santa Barbara Basin, California. *Limnology and Oceanography*, 35(7), 1577-1585.

Robinson, R. S., Kienast, M., Luiza A. A., Altabet, M., Contreras, S., De Pol Holz, R., et al. (2012). A review of nitrogen isotopic alteration in marine sediments. *Paleoceanography*, 27, PA4203. https://doi.org/10.1029/2012PA002321

Santa Barbara County http://www.countyofsb.org/pwd/rainhistory.sbc, Latest Access: October 15, 2018.

Sarno, C., Benitez-Nelson, C.R., Ziolkowski, L., Hendy, I.L., & Thunell, R.C. (this issue) A 2,000 year record of isotopic and biomarker identification of flood sediments in Santa Barbara Basin, California

Schmittner, A., & Lund, D. C. (2015). Early deglacial Atlantic overturning decline and its role in atmospheric CO_2 rise inferred from carbon isotopes ($\delta^{13}C$). *Climates of the Past*, 11(2), 135-152. https://doi.org/10.5194/cp-11-135-2015.

Seo, H., Brink K. H., Dorman C. E., Koracin, D., & Edwards C. A. (2012). What determines the spatial pattern in summer upwelling trends on the U.S. West Coast? *Journal of Geophysical Research: Oceans*, 117(C8). https://doi.org/10.1029/2012JC008016

Shapiro, S.S. & Wilk, M.B. (1965) An analysis of variance tests for normality (complete samples), *Biometrika*, 52(4): 591-611.

Shuman, F. R., & Lorenzen C. J. (2003). Quantitative degradation of chlorophyll by a marine herbivore. *Limnology and Oceanography*, 20(4), 580-586.

Sigman, D. M., Altabet, M. A., Michener, R., McCorkle, D. C., Fry, B., & Holmes, R. M. (1997). Natural abundance-level measurement of the nitrogen isotopic composition of oceanic nitrate: an adaptation of the ammonia diffusion method. *Marine Chemistry*, 57(3), 227-242.

Sigman, D.M., & Casciotti, K. L. (2001). Nitrogen isotopes in the ocean. In *Encyclopedia of Ocean Sciences* (pp. 40-54). London, Academic Press.

Sigman, D., Robinson, R., Knapp, A., Van Geen, A., McCorkle, D., Brandes, J., & Thunell, R. (2003). Distinguishing between water column and sedimentary denitrification in the Santa Barbara Basin using the stable isotopes of nitrate. *Geochemistry, Geophysics, Geosystems*, 4(5), 1040-1060.

Sigman, D.M., DiFiore, P., Hain, M.P., Deutsch, C., Wang, Y., Karl, D.M., Knapp, A.N., Lehmann, M.F. & Pantoja, S. (2009) The dual isotopes of deepnitrate as a constraint on the cycle and budget of oceanic fixed nitrgoen. *Deep-Sea Research I*, 56: 1419-1439.

Somes, C. J., Schmittner, A., Muglia, J. & Oschlies, A. (2017), A three-dimensional model of the marine nitrogen cycle during the Last Glacial Maximum constrained by sedimentary isotopes. *Frontiers in Marine Science*, 4(108). https://doi.org/10.3389/fmars.2017.00108

Stramma, L., Johnson, G. C., Firing, E., & Schmidtko, S. (2010a). Eastern Pacific oxygen minimum zones: Supply paths and multidecadal changes. *Journal of Geophysical Research: Oceans*, 115(C9). https://doi.org/10.1029/2009JCC005976

Stramma, L., Johnson, G. C., Sprintall, J., & Mohrholz, V. (2008). Expanding Oxygen-Minimum Zones in the tropical oceans. *Science*, 320(5876), 655-658.

Stramma, L., Prince, E. D., Schmidtko, S., Luo, J., Hoolihan, J. P., Visbeck, M. et al. (2012). Expansion of oxygen minimum zones may reduce available habitat for tropical pelagic fishes. *Nature Climate Change*, 2(1), 33-37.

Stramma, L., Schmidtko, S., Levin, L. A., & Johnson, G. C. (2010b). Ocean oxygen minima expansions and their biological impacts. *Deep Sea Research Part I: Oceanographic Research Papers*, 57(4), 587-595.

Sweeney, R. E., & Kaplan, I. R. (1980). Natural abundances of ^{15}N as a source indicator for near-shore marine sedimentary and dissolved nitrogen. *Marine Chemistry*, 9(2), 81-94.

Sydeman, W., García-Reyes, M., Schoeman, D., Rykaczewski, R., Thompson, S., Black, B., & Bograd, S. (2014). Climate change and wind intensification in coastal upwelling ecosystems. *Science*, 345(6192), 77-80.

Talley, L. D. (1993). Distribution and formation of North Pacific intermediate water. *Journal of Physical Oceanography*, 23(3), 517-537.

Dr. Pieter Tans, NOAA/ESRL, www.esrl.noaa.gov/gmd/ccgg/trends/, Latest Access: October 30, 2018.

Tems, C. E., Berelson, W. M., & Prokopenko, M. G. (2015). Particulate $\delta^{15}N$ in laminated marine sediments as a proxy for mixing between the California Undercurrent and the California Current: a proof of concept. *Geophysical Research Letters*, 42(2), 419-427.

Thunell, R. C. (1998). Particle fluxes in a coastal upwelling zone: sediment trap results from Santa Barbara Basin, California. *Deep Sea Research Part II: Topical Studies in Oceanography*, 45(8-9), 1863-1884.

Thunell, R. C., & Kepple, A. B. (2004). Glacial-Holocene $\delta^{15}N$ record from the Gulf of Tehuantepec, Mexico: Implications for denitrification in the eastern equatorial Pacific and changes in atmospheric N_2O. *Global Biogeochemical Cycles*, 18(1). https://doi.org/10.1029/2002GB002028

Thunell, R. C., Benitez-Nelson, C., Varela, R., Astor, Y., & Muller-Karger, F. (2007). Particulate organic carbon fluxes along upwelling-dominated continental margins: Rates and mechanisms. *Global Biogeochemical Cycles*, 21, GB1022. https://doi.org/10.1029/2006GB002793

Tiselius, P. & Fransson, K. (2016). Daily changes in $\delta^{15}N$ and $\delta^{13}C$ isotopes in copepods: equilibrium dynamics and variations of trophic level in the field. *Journal of Plankton Research*, 38(3), 751-761.

Varela, R., Álvarez, I., Santos, F., deCastro, M., & Gómez-Gesteira, M. (2015). Has upwelling strengthened along worldwide coasts over 1982-2010? *Scientific Reports*, 5, 10016. https://doi.org/10.1038/srep10016

Voss, M., Altabet, M.A., & Bodungen, B. (1996) $\delta^{15}N$ in sedimenting particles as indicator of euphotic-zone processes, *Deep-Sea Research I*, 43(1): 33-47.

Voss, M., Dippner, J. W., & Montoya, J. P. (2001). Nitrogen isotope patterns in the oxygen-deficient waters of the Eastern Tropical North Pacific Ocean. *Deep Sea Research Part I: Oceanographic Research Papers*, 48(8), 1905-1921.

Wang, Y., Hendy, I., & Thunell, R. (*this issue*), Local and remote forcing of denitrification in the Northeast Pacific for the last 2000 years.

Yang, S., Gruber, N., Long Matthew, C., & Vogt, M. (2017). ENSO-Driven Variability of Denitrification and Suboxia in the Eastern Tropical Pacific Ocean. *Global Biogeochemical Cycles*, 31(10), 1470-1487.

Zhang, C. L., Huang, Z., Cantu, J., Pancost, R. D., Brigmon, R. L., Lyons, T. W., & Sassen, R. (2005). Lipid biomarkers and C\carbon isotope signatures of a microbial (Beggiatoa) mat associated with gas hydrates in the Gulf of Mexico. *Applied Environmental Microbiology*, 71(4), 2106-2112.

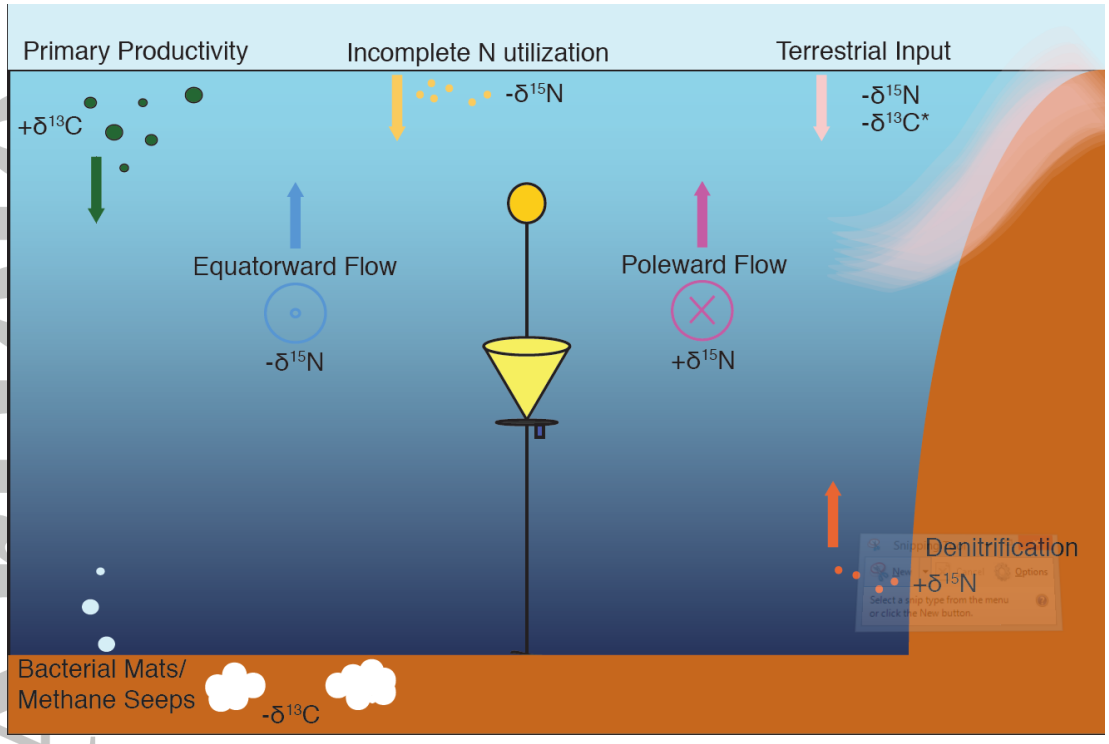

Figure 1. Cartoon depicting the major drivers of $\delta^{15}N$ and $\delta^{13}C_{org}$ in SBB. Upward arrows indicate sources of $\delta^{15}N$ delivered to surface waters, and downward arrows export of $\delta^{15}N$ and $\delta^{13}C_{org}$ signals to the sediment. The influence of terrestrial $\delta^{13}C_{org}$ is noted with an asterisk. In most systems terrestrial organic carbon would be associated with higher $\delta^{13}C_{org}$, however recent analyses of $\delta^{13}C_{org}$ in local river sediments shows that the terrestrial end member may be closer to typical marine values (Sarno et al., *this issue*).

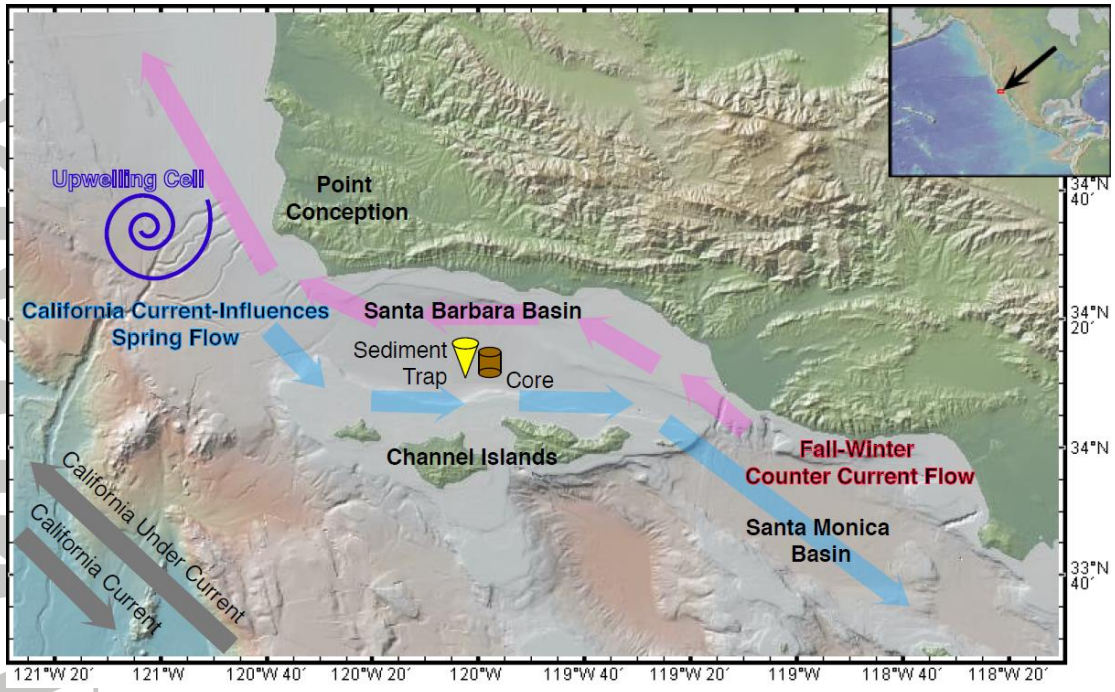

Figure 2. Map of Santa Barbara Basin and the surrounding region, showing the location of the sediment trap time series and core location.

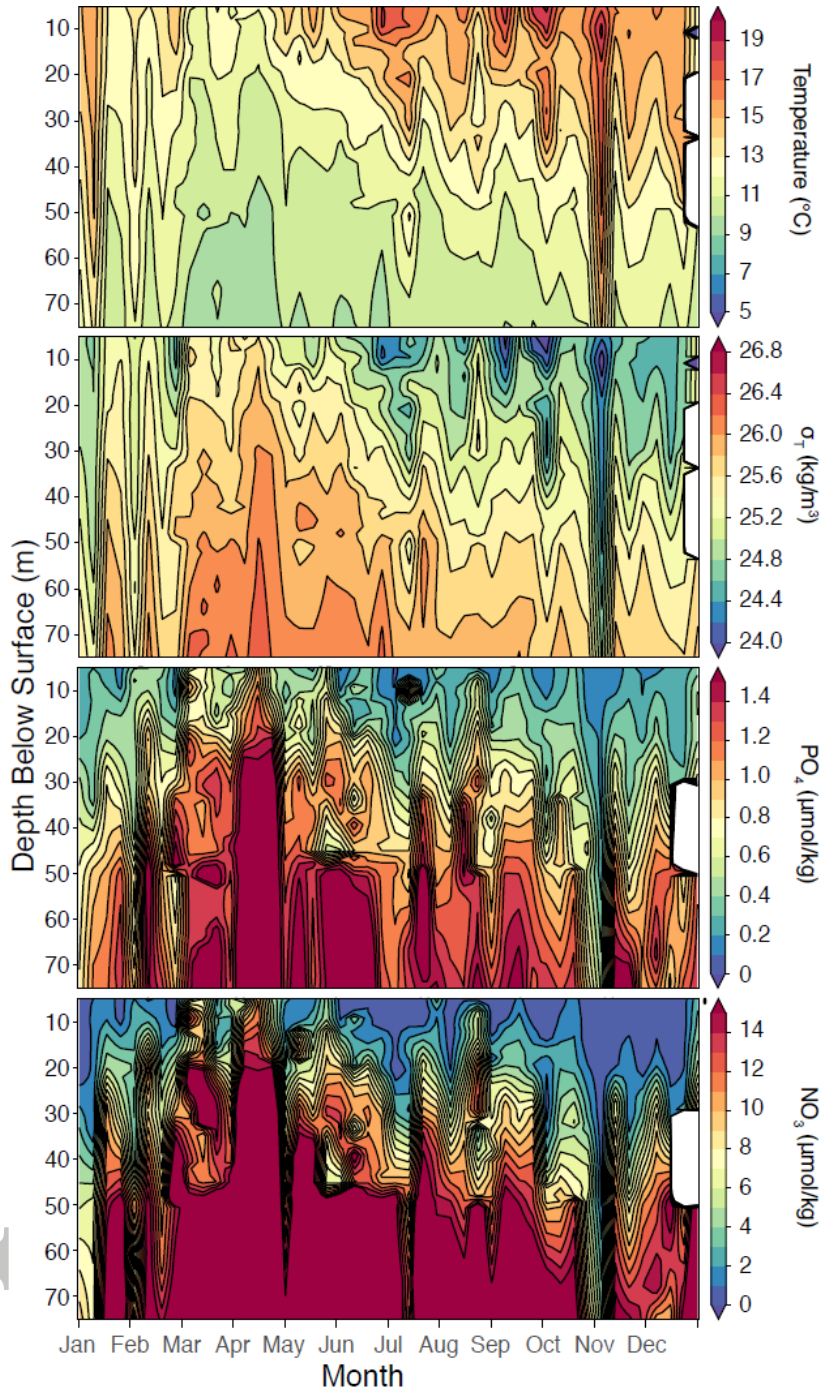

Figure 3. Conditions in Santa Barbara Basin derived from monthly Plumes and Blooms bottle data between 1996 and 2016 plotted by day of the year. Plots show from top to bottom, temperature, σ_T, PO_4 concentrations (µmol/kg), and the concentration of NO_3 ($(NO_3+NO_2) - NO_2$) (µmol/kg).

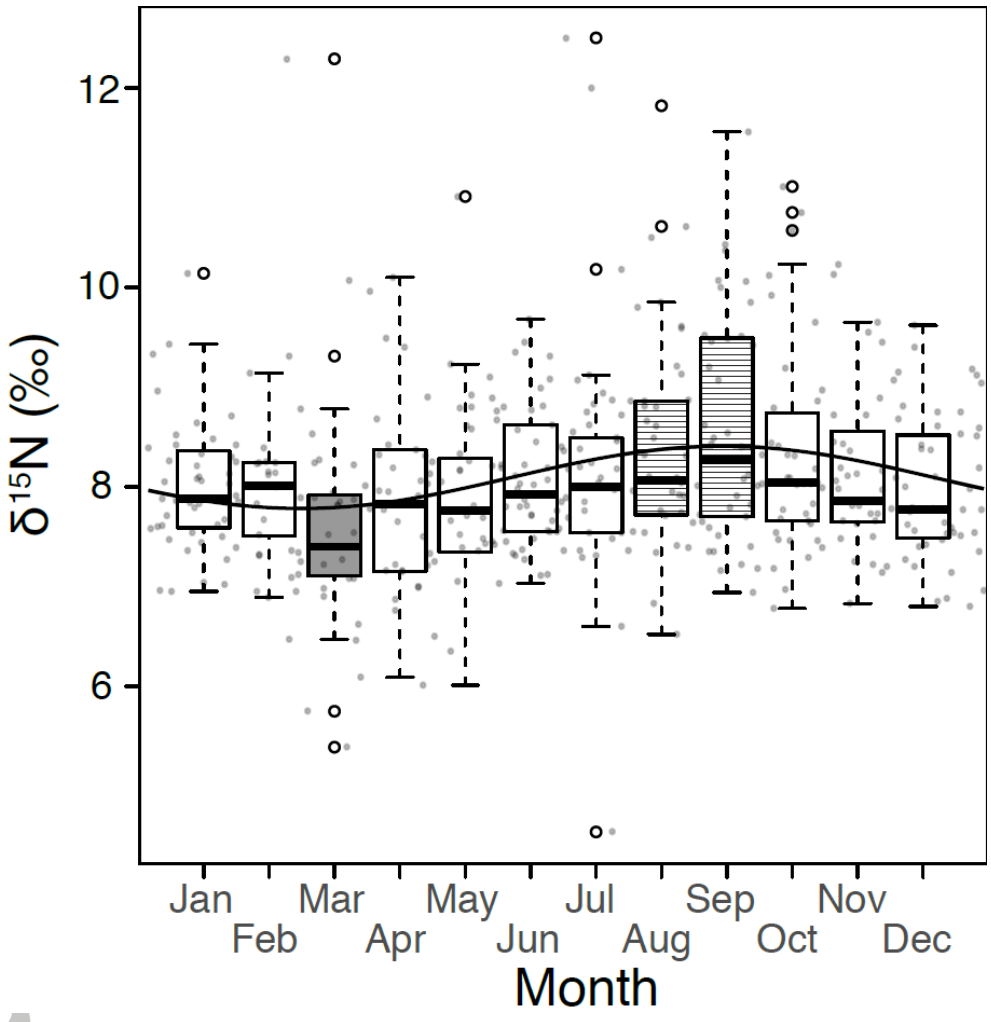

Figure 4. Boxplots of seasonal $\delta^{15}N$ flux to the SBB sediment trap. Months that are significantly different from one another are denoted by light and dark gray shading (Shapiro-Wilks; Dunn's post-hoc test; $p < 0.05$). The black bar denotes the median in each month and the boxes denote the 1st and 3rd quartiles. Superimposed on the boxplot are all available $\delta^{15}N$ data (gray points) as well as a periodic regression describing observed seasonality ($r^2 = 0.05$, $p < 0.001$).

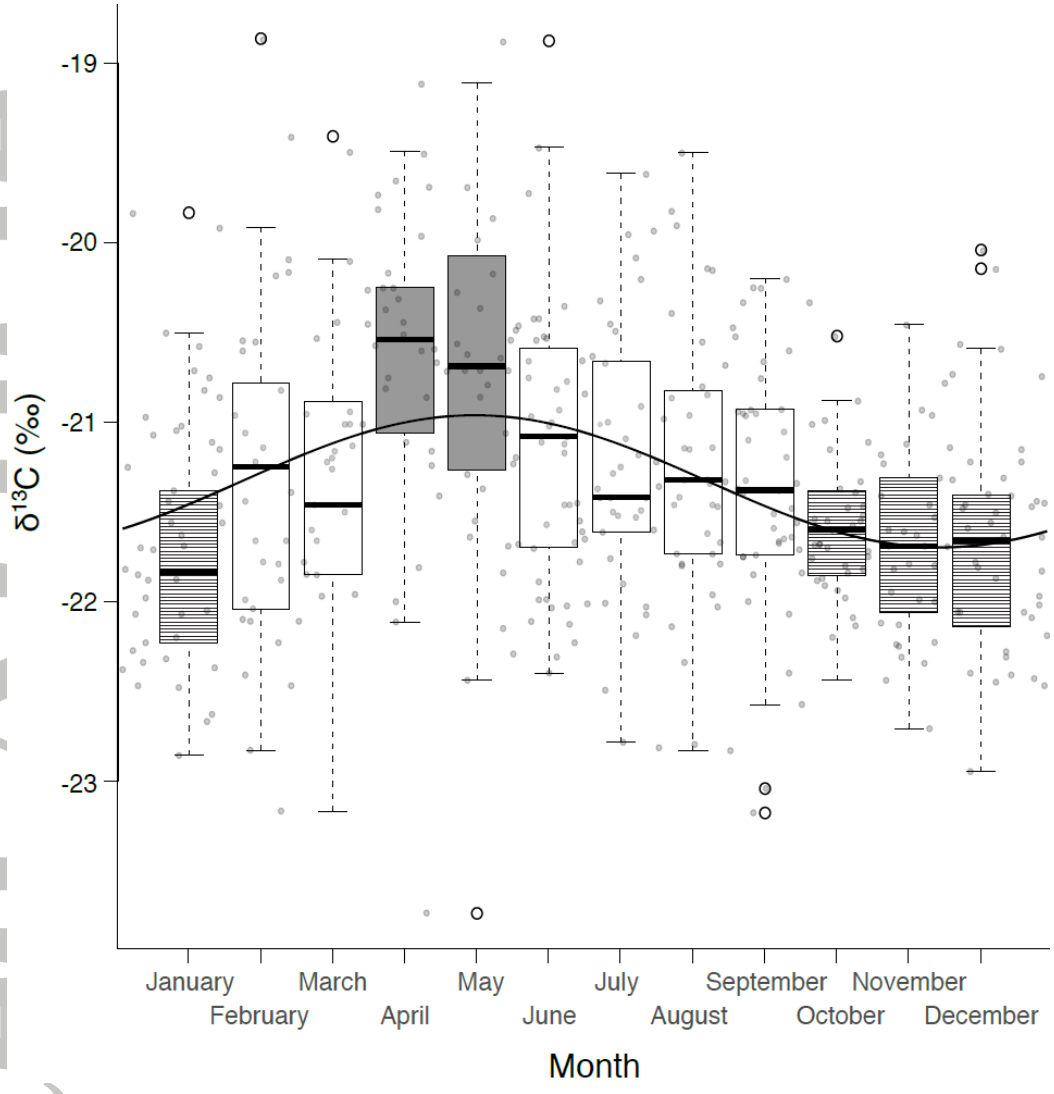

Figure 5. Boxplots of seasonal $\delta^{13}C_{org}$ flux to the SBB sediment trap. The black bar denotes the median value for each month and the boxes denote the 1st and 3rd quartiles. Months that are significantly different from one another are denoted by light and dark gray shading (Shapiro-Wilks; Dunn's post-hoc test; $p < 0.05$). Superimposed on the boxplot are all available $\delta^{13}C_{org}$ data (gray points) as well as a periodic regression describing observed seasonality ($r^2 = 0.11$, $p < 0.001$).

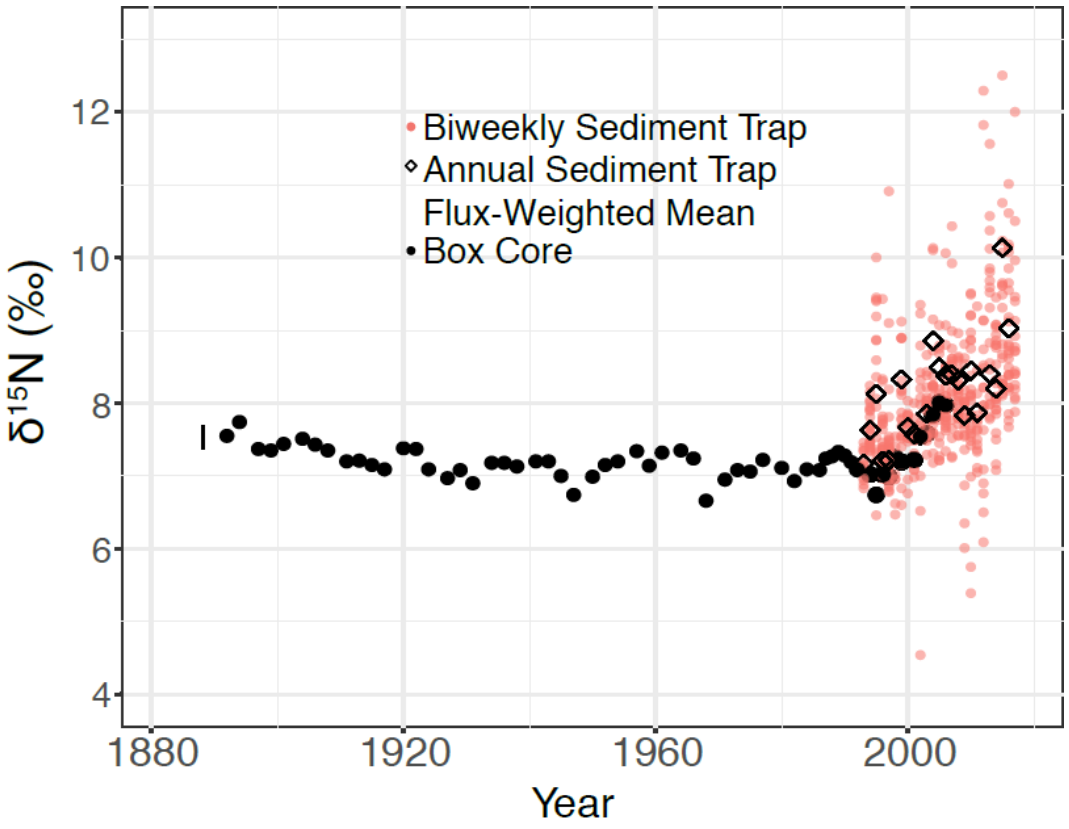

Figure 6. Compilation of all sediment trap $\delta^{15}N$ (open pink circles), flux weighted annual mean sediment trap values (open diamonds) and sediment core values (black circles) from 1892 to 2017. The error bar shown to the left of data is based on the maximum difference between replicate samples.

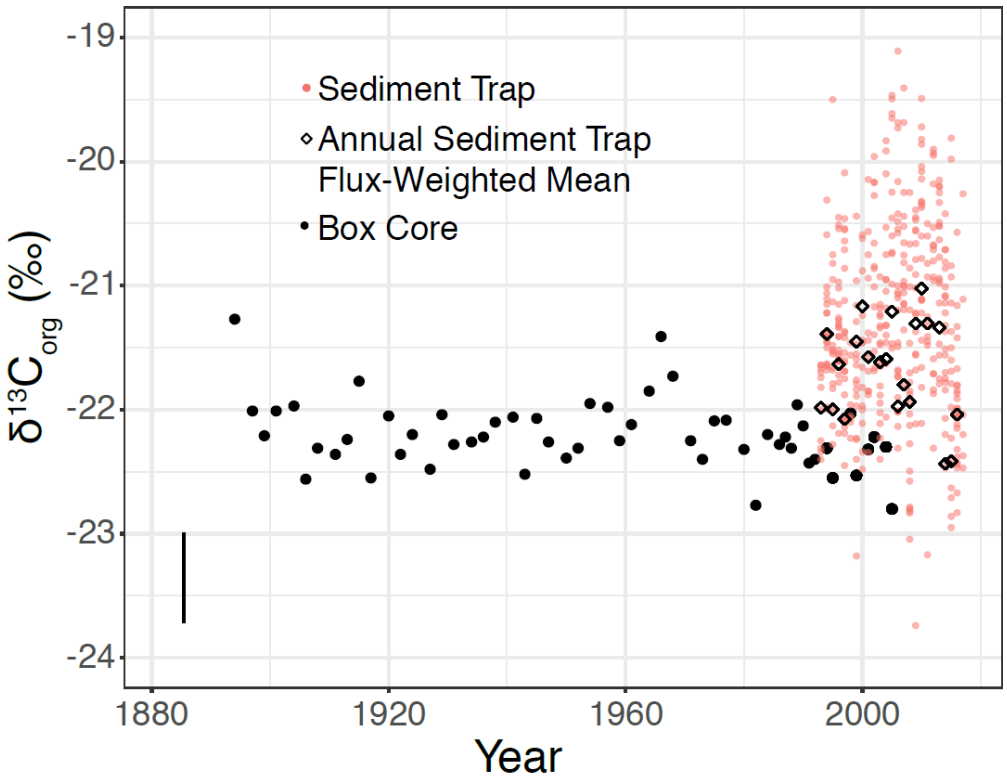

Figure 7. Compilation of all sediment trap $\delta^{13}C_{org}$ (open pink circles), flux weighted annual mean sediment trap values (open diamonds) and sediment core values (black circles) from 1892 to 2017. The error bar shown to the left of data is based on the maximum difference between replicate samples.

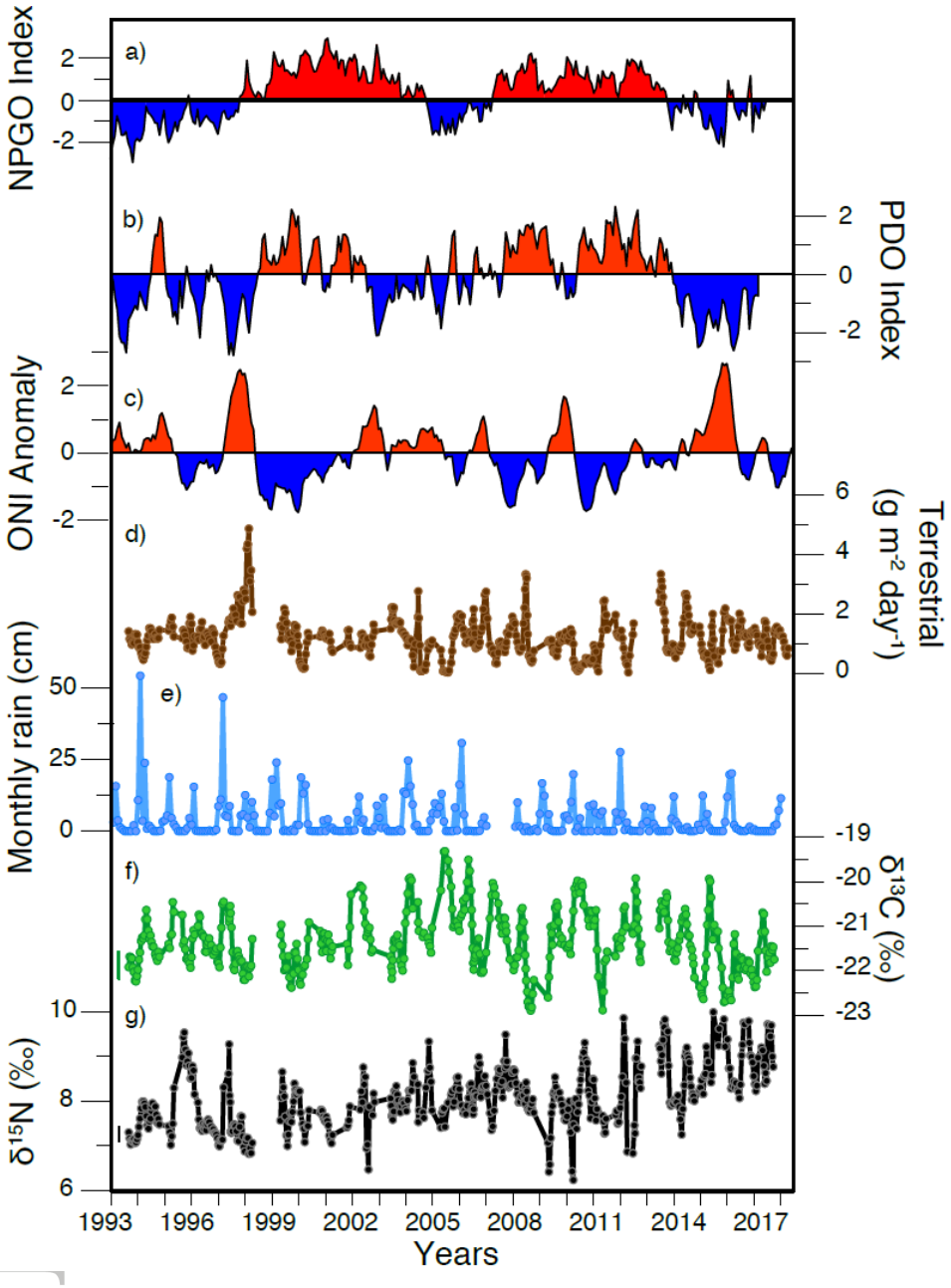

Figure 8. Time series of a) the NPGO index b) the PDO index, c) the Oceanic Niño Index (ONI) anomaly, d) terrestrial flux g m^{-2} day^{-1} from the SBB sediment trap, e) monthly rainfall data for Santa Barbara county (cm), f) $\delta^{13}C_{org}$, and g) $\delta^{15}N$ time series from the SBB sediment trap. The error bars shown to the left of $\delta^{13}C_{org}$ and $\delta^{15}N$ are based on the maximum difference between replicate samples.

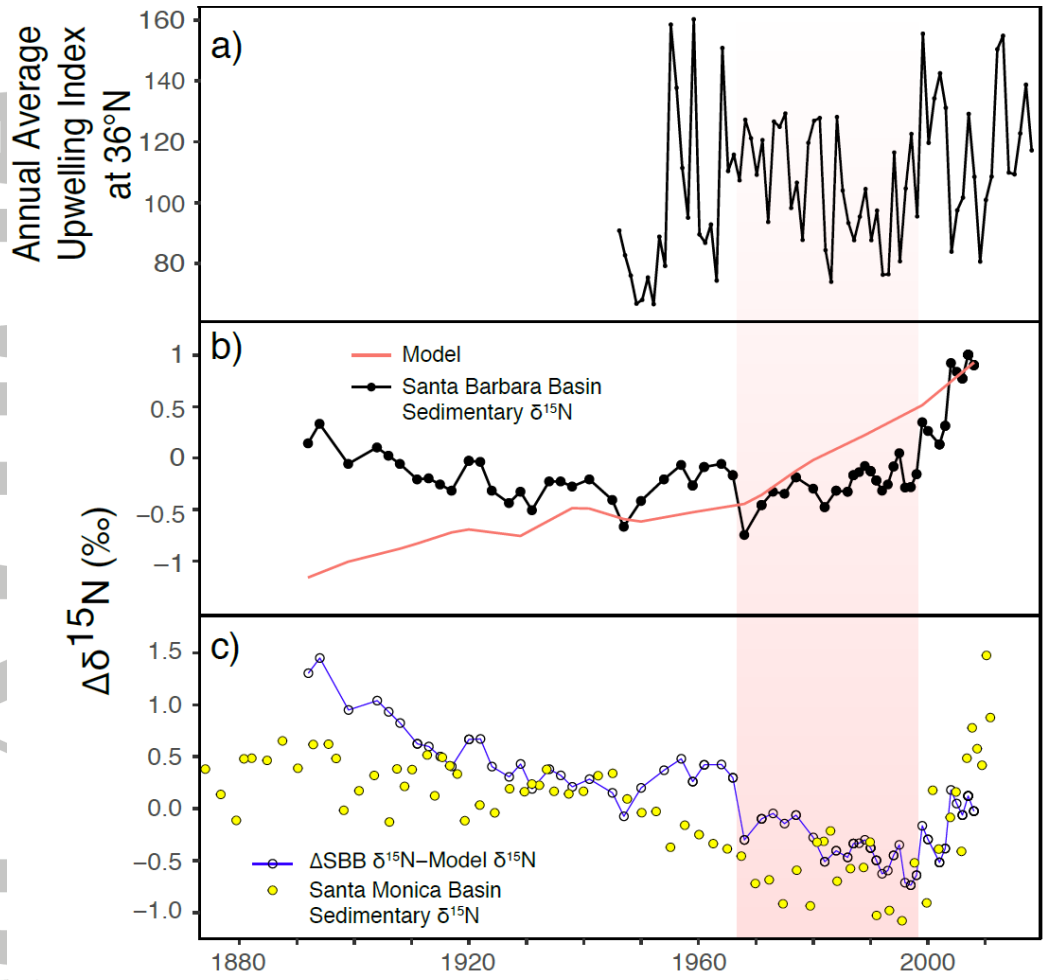

Figure 9. Comparison of (a) annual average upwelling index (PFEL) for 36°N, (b) modeled output of anthropogenically-driven changes in the $\delta^{15}N$ of nitrate in the ETNP (90°W, 10°N, 25m; red line) and the combined series of bulk $\delta^{15}N$ flux in the SBB sediment core and annually flux weighted trap materials (black). Below is (c) the difference between the SBB record and modeled output (open black circles on blue) along with data from the Santa Monica Basin (closed yellow circles; Tems et al., 2015), which is representative of other records from the Eastern Pacific Margin south of SBB. All $\delta^{15}N$ records have been subtracted from the long-term mean for direct comparison. The period of reduced equatorial trade wind activity and upwelling north of Point Conception is denoted by the shaded region.